This paper is published as part of a PCCP Themed Issue on:
Solid-State NMR Spectroscopy

Guest Editors: Paul Hodgkinson, Durham, UK, and Stephen Wimperis, Glasgow, UK

Editorial

Perspectives

Papers

Calculation of fluorine chemical shift tensors for the interpretation of oriented ^{19}F-NMR spectra of gramicidin A in membranes
Ulrich Sternberg, Marco Klipfel, Stephan L. Grage, Raiker Witter and Anne S. Ulrich, *Phys. Chem. Chem. Phys.*, 2009
DOI: 10.1039/b908236k

***J*-Based 3D sidechain correlation in solid-state proteins**
Ye Tian, Lingling Chen, Dimitri Niks, J. Michael Kaiser, Jinfeng Lai, Chad M. Rienstra, Michael F. Dunn and Leonard J. Mueller, *Phys. Chem. Chem. Phys.*, 2009
DOI: 10.1039/b911570f

Natural abundance ^{13}C and ^{15}N solid-state NMR analysis of paramagnetic transition-metal cyanide coordination polymers
Pedro M. Aguiar, Michael J. Katz, Daniel B. Leznoff and Scott Kroeker, *Phys. Chem. Chem. Phys.*, 2009
DOI: 10.1039/b907747b

New opportunities in acquisition and analysis of natural abundance complex solid-state ^{33}S MAS NMR spectra: $(CH_3NH_3)_2WS_4$†

Hans J. Jakobsen,*[a] Henrik Bildsøe,[a] Jørgen Skibsted,[a] Michael Brorson,[b] Bikshandarkoil R. Srinivasan,[c] Christian Näther[d] and Wolfgang Bensch[d]

Received 9th March 2009, Accepted 29th April 2009
First published as an Advance Article on the web 5th June 2009
DOI: 10.1039/b904841n

Population transfer from the satellite transitions to the central transition in solid-state ^{33}S MAS NMR, employing WURST inversion pulses, has led to detection of the most complex ^{33}S MAS NMR spectrum observed so far. The spectrum is that of $(CH_3NH_3)_2WS_4$ and consists of three sets of overlapping resonances for the three non-equivalent S atoms, in accord with its crystal structure. It has been fully analyzed in terms of three sets of ^{33}S quadrupole coupling and anisotropic/isotropic chemical shift parameters along with their corresponding set of three Euler angles describing the relative orientation of the tensors for these two interactions. The three sets of spectral parameters have been assigned to the three different sulfur sites in $(CH_3NH_3)_2WS_4$ by relating the changes observed for the spectral parameters to the changes in crystal structures in a comparison with the corresponding data for the isostructural $(NH_4)_2WS_4$ analog.

Introduction

Sulfur, oxygen, and nitrogen constitute the most important light elements in a large number of inorganic-, organic-, and bio-materials if one leaves out the two common elements carbon and hydrogen. While NMR detection of the spin-1/2 ^{15}N isotope is performed routinely in multidimensional (1D, 2D and 3D) experiments, mainly due to the availability of moderately inexpensive ^{15}N-labelled materials, detection of the three quadrupolar spin isotopes ^{14}N, ^{17}O and ^{33}S can be much more difficult, particularly in solid-state NMR. In recent years, applications of solid-state ^{14}N and ^{17}O MAS NMR methods have increased considerably, first of all because of improved NMR instrumentations and in the case of ^{17}O, an increasing use of relatively inexpensive ^{17}O-labelled materials. In contrast, the field of solid-state ^{33}S MAS NMR spectroscopy lacks much behind because of the low natural abundance (0.76%) and low γ for the ^{33}S (spin $I = 3/2$) quadrupole nucleus. Coupled with the extremely high costs of isotopically ^{33}S-enriched materials, these are the reasons why only about ten articles involving solid-state ^{33}S MAS NMR have been published.[1–10] Most of these studies concern ^{33}S MAS NMR spectra of rather simple inorganic sulfates and sulfides for which analysis requires consideration of only the quadrupole interaction with fairly small quadrupolar coupling constants (C_Q) (^{33}S chemical shift anisotropies are negligibly small in these compounds) and only for a single unique sulfur site in the asymmetric unit of their crystal structures.[2–7] However, most recently quadrupolar coupling constants up to $C_Q \sim 9$ MHz, in layered transition metal sulfides, have been determined from solid-state static ^{33}S NMR spectra acquired at ultra high magnetic fields using the QCPMG pulse sequence.[10]

With ^{33}S being the nearest neighbour to ^{14}N (spin $I = 1$) in the periodic table of NMR frequencies, we have recently taken advantage of the experimental/instrumental experiences gained during the past decade from our ^{14}N MAS NMR studies[11,12] as means for improvements within ^{33}S MAS NMR.[6,8] Most importantly, we recently introduced the techniques of population transfer (PT) for sensitivity enhancement in natural abundance ^{33}S MAS NMR by employing a pair of inversion pulses, either HS (hyperbolic secant) or WURST (wide band uniform rate smooth truncation) pulses, to the spinning side bands (ssbs) of the ^{33}S satellite transitions (STs).[9] Thereby, signal enhancements by a factor in the range 1.74–2.25 were observed for the ^{33}S central transition (CT). This corresponds to a saving in spectrometer time by a factor up to five, a time saving that is extremely welcome in ^{33}S MAS NMR studies. It is noted that enhancement techniques in solid-state NMR of quadrupolar nuclei such as DFS (double frequency sweep),[13] RAPT (rotor assisted population transfer),[14] HS pulses,[15] and WURST[16] have been extensively investigated during the past decade employing more commonly and easier accessible quadrupolar nuclei (*e.g.*, ^{23}Na, ^{27}Al, ^{87}Rb).

This study presents acquisition and complete analysis of what is the most complex natural abundance ^{33}S MAS NMR spectrum acquired and analyzed so far. It clearly illustrates the advancements that is achieved and should serve as an appetizer for future applications of solid-state ^{33}S NMR within chemistry and materials research. The spectrum is that of polycrystalline bis(methylammonium) tetrathiotungstate,

[a] *Instrument Centre for Solid-State NMR Spectroscopy, Department of Chemistry, Aarhus University, Aarhus C, DK-8000, Denmark. E-mail: hja@chem.au.dk*
[b] *Haldor Topsøe A/S, Nymøllevej 55, Lyngby, DK-2800, Denmark*
[c] *Department of Chemistry, Goa University, Goa, 403206, India*
[d] *Institut für Anorganische Chemie, Universität Kiel, D-24098, Kiel, Germany*

† Electronic supplementary information (ESI) available: Differences in crystal structures for $(CH_3NH_3)_2WS_4$ and $(NH_4)_2WS_4$ from X-ray diffraction. Comparison of the ^{33}S chemical shift tensors with the ^{77}Se and ^{17}O tensors for $(NH_4)_2WSe_4$ and K_2WO_4. See DOI: 10.1039/b904841n

$(CH_3NH_3)_2WS_4$, and is obtained for ^{33}S in natural abundance employing the WURST PT method.[9]

Experimental

Synthesis

Bis(methylammonium) tetrathiotungstate, $(CH_3NH_3)_2WS_4$, was obtained as yellow crystals when $(NH_4)_2WS_4$ (1 g) is dissolved in H_2O (2 mL) and 40% methylamine, CH_3NH_2, (5 mL) and then filtered and allowed to crystallize for one day as recently described.[17] Identity was checked by X-ray diffraction[17] and by ^{33}S MAS NMR spectroscopy as performed in the present article.

NMR spectroscopy

The ^{33}S MAS NMR experiments were performed at 46.04 MHz on a Varian Direct Drive VNMRS-600 spectrometer equipped with an Oxford Instruments 14.1 T wide-bore magnet. The experiments employed a Varian Chemagnetics double-resonance T3® MAS probe for 7.5 mm rotors. The magic angle of $\theta = 54.736^\circ$ was adjusted to the highest possible precision ($< \pm 0.005^\circ$) by ^{14}N MAS NMR at the nearby frequency of 43.34 MHz, using e.g. a sample of $Pb(NO_3)_2$, as recently described.[6] The sample of $(CH_3NH_3)_2WS_4$ was spun at a MAS frequency of $\nu_r = 5500$ Hz with an ultrahigh precision (< 0.5 Hz) in ν_r, employing the experimental setup combined with a Varian/Chemagnetic MAS speed controller as recently described.[18] Rf field strengths were calibrated for different transmitter power levels using a sample of neat CS_2. Usually a rf field strength of about 13 kHz (*i.e.*, a pulse width of 19.5 μs for a 90° flip angle) was used for both the population transfer (PT) inversion pulses and excitation of the PT enhanced and standard magnetizations. For the excitation of the magnetization to be observed, a pulse width of 5.0 μs, *i.e.* corresponding to a flip angle of 23°, was employed. Since it has been demonstrated elsewhere[6] that ^1H decoupling of residual ^{33}S–^1H dipolar couplings in ^1H-containing samples is required only for spinning frequencies $\nu_r < 2000$ Hz, ^1H decoupling was not employed for the present sample ($\nu_r = 5500$ Hz). The ^{33}S chemical shifts are referenced to the ^{33}S resonance for the sample of neat CS_2, the standard ^{33}S chemical shift reference. The offset values for the two WURST PT inversion pulses applied to the two ^{33}S ($\pm 3/2 \leftrightarrow \pm 1/2$) satellite transitions (STs)[9] should preferably be set in the region of the two "horns" for the STs. This has recently been evaluated by Wasylishen and co-workers, using hyperbolic secant (HS) pulses for PT enhancements of the central transitions (CTs) in simple inorganic compounds containing quadrupolar nuclei of high NMR sensitivity (*e.g.*, ^{87}Rb and ^{27}Al), and with well-known quadrupolar coupling parameters.[15] Furthermore, with the exceptions of very small ^{33}S quadrupole coupling constants (C_Q) and asymmetry parameters (η_Q) approaching the value of one, this evaluation has been fully confirmed by our exploratory WURST/HS PT enhancement study for natural abundance ^{33}S MAS NMR.[9] Because the ^{33}S C_Q and η_Q parameters are unknown for the title compound of this study, $(CH_3NH_3)_2WS_4$, the two WURST PT inversion pulses employed here used the same slightly asymmetrically displaced offsets (120.8 kHz and −107.2 kHz) as used recently[9] for the corresponding ammonium compound, $(NH_4)_2WS_4$, assuming fairly similar C_Q, η_Q parameters. As also has been evaluated by Wasylishen and co-workers for the HS PT experiment,[15] the bandwidth (bw) of the WURST inversion pulses was set equal to the spinning frequency $\nu_r = 5500$ Hz in order for the individual inversion pulse to cover the full width (lineshape) of a single ssb within a ST, independent of the value chosen for the offset. The pulse length (T_p) for the WURST inversion pulses was set equal to $T_p = 8$ ms, a typical value used in HS and WURST PT enhancement experiments,[9,15] and was not subjected to optimization for maximum enhancement because generally only minor changes are observed by variation of this parameter, *e.g.* in the range $T_p = 4$–12 ms.[9]

The WURST pulse shapes were generated using the spectrometer system Wave Form Generator (WFG) hardware option along with either Varian's "Pandora Box" software package or by direct programming of the individual preparatory pulse elements. The two offset values used for the inversion pulses were generated by either cosine amplitude modulation (symmetrical offsets) or phase and amplitude modulation (non-symmetrical offsets) of the WURST pulse shapes.

Spectral analysis

The WURST PT-enhanced natural abundance ^{33}S MAS NMR spectra of the CTs for the three unique S sites within the WS_4^{2-} ion of $(CH_3NH_3)_2WS_4$ have been analyzed using the STARS simulation software package. STARS (spectrum analysis for rotating solids) was developed in our laboratory several years ago[19,20] and the original version of STARS was early on incorporated into Varian's VNMR software for SUN Microsystem computers and has been available from Varian Inc as part of their VNMR Solids software package.[21] The present version of STARS used here has been intensively upgraded during the past few years and is capable of handling spectral parameters (*i.e.*, quadrupole coupling (C_Q, η_Q), chemical shift (δ_{iso}, δ_σ, η_σ), and Euler angles (ψ, χ, ξ) relating the relative orientation for these two interactions) for up to nine different nuclear sites in the optimization of a fit to an experimental spectrum. In addition to these spectral parameters, the program can also include (i) deviation from the magic-angle, (ii) rf bandwidth, (iii) rf offset, (iv) jitter in spinning frequency[18] and (v) the linewidths (Lorentzian and/or Gaussian) in the iterative fitting procedure. This upgraded version of STARS has been incorporated into both the Varian VNMRJ software running on SUN Microsystems Ultra-5 workstations and the VNMRJ software running on a Linux RedHat PC.

The quadrupole coupling and CSA parameters are defined by:

$$C_Q = eQV_{zz}/h;\ \eta_Q = (V_{yy} - V_{xx})/V_{zz} \quad (1)$$

$$\delta_\sigma = \delta_{iso} - \delta_{zz};\ \eta_\sigma = (\delta_{xx} - \delta_{yy})/\delta_\sigma \quad (2)$$

$$\delta_{iso} = (1/3)(\delta_{xx} + \delta_{yy} + \delta_{zz}) = (1/3)\mathrm{Tr}(\delta) \quad (3)$$

using the convention,

$$|\lambda_{zz} - (1/3)\mathrm{Tr}(\lambda)| \geq |\lambda_{xx} - (1/3)\mathrm{Tr}(\lambda)| \geq |\lambda_{yy} - (1/3)\mathrm{Tr}(\lambda)| \quad (4)$$

for the principal elements ($\lambda_{\alpha\alpha} = V_{\alpha\alpha}$, $\delta_{\alpha\alpha}$) of the two tensors. The relative orientation of the two tensors is described by the three Euler angles (ψ, χ, ξ), which correspond to positive rotations of the CSA tensor around δ_{zz} (ψ), the new δ_{yy} (χ), and the final δ_{zz} (ξ) axis.

Results and discussion

The natural abundance WURST PT ^{33}S MAS NMR spectrum of $(CH_3NH_3)_2WS_4$ (I) shown in Fig. 1a has been acquired in 45 h (325 000 scans with a repetition delay of 0.5 s) and exhibits a noise level and resolution that allow even the low-intensity resonances to be properly observed and included in the analysis and fitting of the spectrum. It is important to note that the WURST PT ^{33}S MAS NMR spectrum in Fig. 1a is not the result of several optimizations of experimental parameters, as *e.g.* the two offset values for the WURST inversion pulses and the length (T_p) of these WURST pulses, which could have been very tedious. The Fig. 1a spectrum is simply the result of a qualified estimate of the experimental and spectral parameters based on the data for related compounds in WURST PT ^{33}S enhancement[9] and the results described in general for HS sensitivity enhancement of the more common quadrupolar nuclei.[15] In general we find that the WURST and HS PT enhancement techniques as applied to ^{33}S MAS NMR are very robust to qualified estimates of the experimental parameters employed in the PT pulse sequences. Furthermore, it is noteworthy that an initial single-pulse experiment, in which PT techniques were *not* used, was stopped after 40 h of spectral accumulations because we found the noise level too high to justify a continuation of the experiment. Just as importantly, in this single-pulse spectrum of the CT region the STs interfere with the resonances for CTs and thus further add to the complexity of an already complex spectrum, thereby most likely impeding spectral analysis and an iterative fit. In addition to the gain in sensitivity obtained for the WURST PT spectrum in Fig. 1a, the STs are completely suppressed ('saturated') in this spectrum, which highly favours this experiment (*vide infra*). To obtain an estimate of the signal enhancement factor for the WURST PT ^{33}S MAS NMR spectrum (Fig. 1a), the overall total integrated intensity of that spectrum has been compared with that for the standard single-pulse experiment stopped after almost two days of spectral accumulations, both determined on the same absolute intensity scale. From the total integral of the standard single-pulse spectrum for the CT region, excluding the STs in the CT region, a signal enhancement by a factor of 2.1 (corresponding to a saving in spectrometer time by a factor of 4.4) is achieved employing the WURST PT method, in excellent agreement with the results of our recent study.[9] It is noted that the signal enhancement by a factor of 2 exactly corresponds to 'nulling' (saturation of) the intensity for the STs.

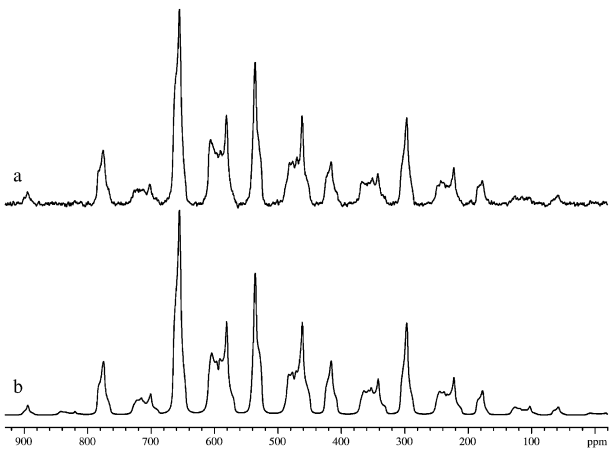

Fig. 1 (a) Natural abundance ^{33}S MAS NMR spectrum of the central transition in $(CH_3NH_3)_2WS_4$ obtained by WURST population transfer at 46.04 MHz and ν_r = 5500 Hz. (b) Corresponding simulated spectrum using the parameters listed in Table 1.

The ^{33}S MAS NMR spectrum of the CT in (I) (Fig. 1a) consists of several bands of resonances, which can be divided into at least two different sets for which the bands within each set are separated by the applied MAS frequency of ν_r = 5500 Hz, *i.e.* spinning side bands (ssbs). Furthermore, each of these ssbs exhibits very complex lineshapes of highly different appearances. Each set of ssbs arises from the chemical shift anisotropy (CSA) interaction for a particular sulfur atom, while the lineshape within the individual ssbs is caused by the second-order quadrupolar interaction for this particular sulfur atom. Following the very recent report on the crystal structure of (I),[17] the WS_4^{2-} ions in the asymmetric unit are all equivalent, while the four sulfur atoms in the WS_4^{2-} ion occupy three unique sites: S(1,1), S(2), and S(3). Thus, the crystal structure is identical to that for $(NH_4)_2WS_4$ (II)[22] and to those for some alkalimetal (Rb and Cs) WS_4^{2-} salts.[23,24] Summation of the integrals for the individual ssbs within the two separated sets of ssbs yields a ratio of 1:1 for the two sums. Thus, the ssb pattern formed by the most narrow ssb lineshapes (*i.e.*, the high-frequency pattern) is assigned to the two equivalent S(1) atoms, while the other more complex ssb pattern (*i.e.*, the pattern at low frequency) must be formed by overlap of two ssb patterns from the S(2) and S(3) atoms.

Spectral analysis of these ssb patterns using STARS is performed in terms of ^{33}S chemical shift (δ_{iso}, δ_σ, η_σ) and quadrupole coupling (C_Q, η_Q) parameters along with the three Euler angles (ψ, χ, ξ) relating the relative orientation for the two tensorial interactions for the three different S sites with the relative intensities of 2 : 1 : 1. Following some preliminary spectral simulations using different sets of parameters for these sites, a final fit of simulated spectra to the experimental spectrum could be initiated. This simultaneous optimization for all three S-sites involved a total of 29 parameters, which were allowed to vary in an overnight run on a Linux RedHat PC. The simulated spectrum corresponding to the optimized parameters summarized in Table 1 is shown in Fig. 1b. The excellent agreement between the experimental and simulated spectra in Fig. 1 is clearly attributable to the very good S/N obtained for the experimental spectrum. The appearances of the individual simulated spectra of the central transition for S(2) and S(3), which heavily overlap in the experimental spectrum, are displayed in Fig. 2b and c, each mixed with a simulation for S(1) in a 1 : 1 ratio. Thus, addition of the spectra in Fig. 2b and c forms the spectrum in Fig. 2a.

In addition to the spectral parameters for (I), Table 1 also lists those determined recently for the isostructural

Table 1 ^{33}S quadrupole coupling (C_Q, η_Q) and chemical shift parameters (δ_σ, η_σ, δ_{iso}) for $(CH_3NH_3)_2WS_4$ (I) determined from WURST PT enhanced natural-abundance ^{33}S MAS NMR spectra and compared to the parameters for $(NH_4)_2WS_4$ (II) determined from standard ^{33}S MAS spectra[8] (see text)[a]

Compound/sites $(CH_3NH_3)_2WS_4$	C_Q/kHz	η_Q	δ_σ/ppm	η_σ	δ_{iso}/ppm	ψ	χ	ξ	Ref.
S(1,1)	794	0.87	401	0.11	545.3	5°	85°	21°	This work
S(2)	847	1.00	344	0.10	473.1	76°	78°	26°	—
S(3)	965	0.40	383	0.25	491.5	94°	89°	1°	—
$(NH_4)_2WS_4$									
S(1,1)	708	0.77	389	0.16	542.3	147°	10°	2°	8
S(2)	531	0.08	380	0.05	495.8	53°	4°	16°	—
S(3)	620	0.14	396	0.35	518.7	87°	47°	73°	—

[a] The error limits for C_Q, η_Q, δ_σ, and η_σ are similar to those published earlier for the standard ^{33}S MAS NMR spectra,[8] *i.e.*, ±0.07 kHz, ±0.05, ±4 ppm, and ±0.05, respectively. The δ_{iso} values are relative to neat CS_2 (the ^{33}S chemical shift of 1.0 M Cs_2SO_4 is 333 ppm relative to CS_2) and include corrections for the second-order quadrupolar shifts. The ψ, χ, ξ Euler angles shown in the table are those directly obtained from the optimized fitting for the individual S-sites. The smallest error limits for these Euler angles are observed for the χ angle and are less than ±6°. The error limits for the ψ and ξ angles are somewhat higher for (I), but much higher and could even be undefined for (II) because of the simultaneous small values of η_Q and η_σ.[28]

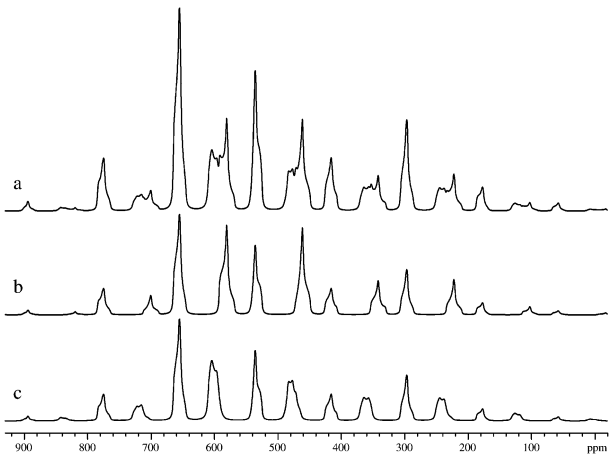

Fig. 2 (a) Simulated spectrum for $(CH_3NH_3)_2WS_4$ shown in Fig. 1b with relative intensities for S(1), S(2) and S(3) equal to 2 : 1 : 1. (b) Simulated spectrum for the S(1) and S(2) sites and (c) the S(1) and S(3) sites, each with relative intensities of 1 : 1. Addition of the spectra in (b) and (c) produces the spectrum in (a).

diammonium salt, $(NH_4)_2WS_4$ (II). Comparison of the changes observed for their spectral parameters coupled with the changes in the crystal structures for (I)[17] and (II)[22] should allow a tentative assignment of the spectral parameters to the S-sites for both (I) and (II). We note that the nomenclature adopted here from the crystal structures for the three different S sites (S(1,1), S(2), S(3)) in Table 1 for both (I) and (II) is identical to that used in the recent report on the crystal structure for (I).[17] The atomic numbering used in the earlier report for the $(NH_4)_2WS_4$ (II) structure,[22] which crystallizes in the same space group as (I), has accordingly been changed to that for (I).

Firstly, the assignment for the two equivalent S(1) atoms in both (I) and (II) follows directly from the above arguments on the analysis for (I) and the data reported for (II).[8,9] The (C_Q, η_Q) and (δ_{iso}, δ_σ, η_σ) spectral parameters determined for the two S(1) sites in (I) and (II) are very much identical (see Table 1). This shows that the structural environments for S(1) in (I) and (II) are quite similar in agreement with the crystal structures for (I)[17] and (II).[22] Secondly, a comparison of the spectral parameters determined for the two remaining S(2) and S(3) sites in (I) and (II) shows that, while the chemical shift parameters (δ_{iso}, δ_σ, η_σ) for these sites in (I) and (II) are very similar, the quadrupole coupling parameters in (I) exhibit quite large increases for both C_Q and η_Q compared to the values in (II). A particular large change is observed for the parameter set C_Q = 847 kHz, η_Q = 1.00, indicating that this set of parameters should be assigned to the S(2)/S(3) atom undergoing the largest change in crystal structure, as judged from a comparison of the differences in crystal structure for (I)[17] and (II)[22] around S(2) and S(3), respectively. The ESI contains information from such a comparison related to the hydrogen bonding network, next-nearest atomic neighbours, W–S bond lengths, and in the form of crystallographic plots for the environments of the S(2) and S(3) sites in (I) and (II).† This has provided clear evidence that the S(2) atom exhibits the largest differences in structural environment between (I) and (II). Thus, assignment of the C_Q = 847 kHz, η_Q = 1.00 parameter set to the S(2) atom completes the assignment of the spectral parameters for (I) (see Table 1). Comparison of the two sets of chemical shift parameters (δ_{iso}, δ_σ, η_σ) and the two C_Q values for the unassigned S(2)/S(3) spectral parameters in (II) with the assigned spectral parameters for (I), immediately gives the convincing assignment shown in Table 1 for the parameters in (II). In particular, we note the overall good agreement between the δ_σ, η_σ, and δ_{iso} values for (I) and (II), which are only slightly affected by the structural differences in contrast to the C_Q, η_Q values for the S(2) and S(3) sites. This is in accordance with the general accepted view that quadrupole coupling parameters are much more sensitive to small changes in structural environments than are chemical shift parameters.

It is clearly of interest to compare the anisotropic and isotropic ^{33}S chemical shift parameters for the three non-equivalent S atoms in the WS_4^{2-} ion of (I) and (II) and their assignments presented above with the corresponding parameters recently reported for the three non-equivalent ^{77}Se (spin I = 1/2) atoms in the WSe_4^{2-} ion of $(NH_4)_2WSe_4$[25]

which is isostructural (*Pnma*)[26] with (I) and (II). Following conversion of the principal axis component (δ_{xx}, δ_{yy}, δ_{zz}) data reported for the ^{77}Se chemical shift parameters[25] to the convention used here (eqn (2)–(4) in the Experimental), this leads us to assign the experimental data reported for $(NH_4)_2WSe_4$ in rows **15b** and **15c** of Table 3 in ref. 25 to the Se(3) and Se(2) sites, respectively, reported for the crystal structure.[26] These sites are identical to the convention used for the S(3) and S(2) sites in the crystal structure of (I)[17] and thus also for (I) and (II) in Table 1, (see also Table 1 in the ESI for the assignment of the ^{77}Se chemical shift parameters for $(NH_4)_2WSe_4$).† Furthermore, it is also noteworthy that the 25 years old ^{17}O isotropic and anisotropic chemical shift data determined for the structurally related (*C*2/*m*) ^{17}O-enriched K_2WO_4 compound[27] conform to the ^{33}S chemical shift parameters reported here (see ESI).†

Finally, it is often argued that an increase in resolution and sensitivity for solid-state MAS NMR spectroscopy of quadrupolar nuclei is achieved by performing experiments at the highest possible magnetic field. The reason is a larger dispersion in chemical shifts combined with narrowing of the second-order quadrupolar lineshapes at higher magnetic field strength. However, this situation could also result in loss of the information contained in the second-order lineshape. To investigate the possible advantage of a very high field for sample (I), a simulation of the spectral appearance at the ultra high magnetic field of 21.15 T (^{1}H at 900 MHz), employing the parameters determined at 14.10 T (Table 1), is performed in Fig. 3. In addition to the increase in sensitivity obtained at the higher magnetic field, this simulation clearly shows the gain in resolution that is achieved by performing the experiment at 21.15 T. However, most importantly these improvements are obtained at the expense of a loss in the information on the quadrupole coupling parameters (C_Q, η_Q) and the three Euler angles (ψ, χ, ξ), parameters which could be determined with good precision from the second-order quadrupolar lineshapes observed for all three S-sites at 14.10 T. Thus, for determination of ^{33}S C_Q, η_Q data any advantage of performing ^{33}S MAS NMR experiments at ultra high magnetic field highly depends on the magnitude of C_Q.

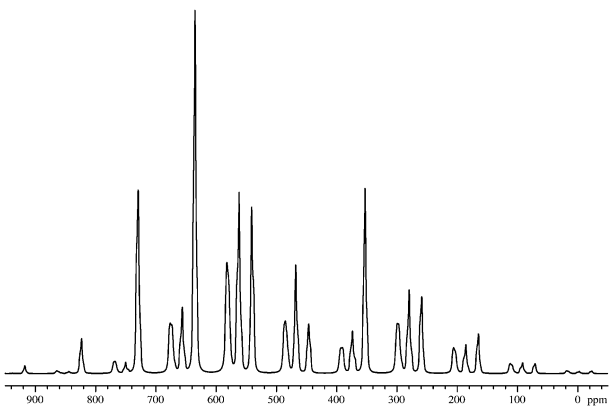

Fig. 3 (a) Simulated ^{33}S MAS NMR spectrum of the central transition in $(CH_3NH_3)_2WS_4$ at 21.15 T (^{33}S at 69.06 MHz or ^{1}H at 900 MHz) and ν_r = 6500 Hz using the parameters in Table 1. The increase in ν_r from 5500 to 6500 Hz for this spectrum is employed to avoid overlap between the three different sets of ^{33}S resonances at this ultra high magnetic field, and thereby to better illustrate the reduction in the second-order quadrupolar line broadening observed at this field.

In conclusion, the present study shows that applying inversion pulses to the satellite transitions, natural abundance ^{33}S MAS NMR spectra of high complexity can be obtained in a reasonable time on a mid-field (14.1 T) spectrometer and with a quality that allows spectral analysis to perfection. Comparison of ^{33}S quadrupole coupling and chemical shift parameters determined for two structurally very similar ammonium tetrathiotungstates has allowed tentative assignments of these parameters to be presented for both compounds based on differences in their crystal structures. Our studies show that natural abundance ^{33}S MAS NMR is now amenable to solving real problems related to sulfur chemistry (*e.g.*, of structural origin). With the option of a ^{33}S-isotope enrichment of just a few percentages, this will greatly enhance possibilities for its applications also in materials sciences.

Acknowledgements

The use of the facilities at the Danish Instrument Centre for Solid-State NMR Spectroscopy, Aarhus University, sponsored by the Danish National Science Research Council, Teknologistyrelsen, Carlsbergfondet and Direktør Ib Henriksens Fond is acknowledged.

References

1 H. Eckert and J. P. Yesinowski, *J. Am. Chem. Soc.*, 1986, **108**, 2140.
2 W. A. Daunch and P. L. Rinaldi, *J. Magn. Reson.*, 1996, **A123**, 219.
3 T. A. Wagler, W. A. Daunch, P. L. Rinaldi and A. R. Palmer, *J. Magn. Reson.*, 2003, **161**, 191.
4 T. A. Wagler, W. A. Daunch, M. Panzer, W. J. Youngs and P. L. Rinaldi, *J. Magn. Reson.*, 2004, **170**, 336.
5 S. Couch, A. P. Howes, S. C. Kohn and M. F. Smith, *Solid State Nucl. Magn. Reson.*, 2004, **26**, 203.
6 H. J. Jakobsen, A. R. Hove, H. Bildsøe and J. Skibsted, *J. Magn. Reson.*, 2006, **180**, 170.
7 J. P. d'Espinose de Lacaillerie, F. Barberon, B. Bresson, P. Fonollosa, H. Zanni, V. E. Fedorov, N. G. Naumov and Z. Gan, *Cem. Concr. Res.*, 2006, **36**, 1781.
8 H. J. Jakobsen, A. R. Hove, H. Bildsøe, J. Skibsted and M. Brorson, *Chem. Commun.*, 2007, 1629.
9 M. R. Hansen, M. Brorson, H. Bildsøe, J. Skibsted and H. J. Jakobsen, *J. Magn. Reson.*, 2008, **190**, 316.
10 A. Sutrisno, V. V. Terskikh and Y. Huang, *Chem. Commun.*, 2009, 186.
11 H. J. Jakobsen, H. Bildsøe, J. Skibsted and T. Giavani, *J. Am. Chem. Soc.*, 2001, **123**, 5098.
12 A. R. Hove, H. Bildsøe, J. Skibsted, M. Brorson and H. J. Jakobsen, *Inorg. Chem.*, 2006, **45**, 10873, and references cited therein..
13 A. P. M. Kentgens and R. Verhagen, *Chem. Phys. Lett.*, 1999, **300**, 435.
14 Z. Yao, H.-T. Kwak, D. Sakellariou, L. Emsley and P. J. Grandinetti, *Chem. Phys. Lett.*, 2000, **327**, 85.
15 (*a*) R. Siegel, T. T. Nakashima and R. E. Wasylishen, *Chem. Phys. Lett.*, 2004, **388**, 441; (*b*) R. Siegel, T. T. Nakashima and R. E. Wasylishen, *J. Magn. Reson.*, 2007, **184**, 85.
16 K. K. Dey, S. Prasad, J. T. Ash, M. Deschamps and P. J. Grandinetti, *J. Magn. Reson.*, 2007, **185**, 326.
17 B. R. Srinivasan, C. Näther and W. Bensch, *Acta Crystallogr., Sect. E: Cryst. Struct. Rep. Online*, 2008, **64**, m296.

18 H. J. Jakobsen, A. R. Hove, H. Bildsøe, J. Skibsted and M. Brorson, *J. Magn. Reson.*, 2007, **185**, 159.
19 H. J. Jakobsen, J. Skibsted, H. Bildsøe and N. C. Nielsen, *J. Magn. Reson.*, 1989, **85**, 173.
20 J. Skibsted, N. C. Nielsen, H. Bildsøe and H. J. Jakobsen, *J. Magn. Reson.*, 1991, **95**, 88.
21 Varian Manual, STARS (SpecTrum Analysis for Rotating Solids), Publication No.87-195233-00, Rev. A0296, 1996.
22 B. R. Srinivasan, M. Poisot, C. Näther and W. Bensch, *Acta Crystallogr., Sect. E: Cryst. Struct. Rep. Online*, 2004, **E60**, i136.
23 J. Yao and J. A. Ibers, *Acta Crystallogr., Sect. E: Cryst. Struct. Rep. Online*, 2004, **60**, i10.
24 B. R. Srinivasan, C. Näther and W. Bensch, *Acta Crystallogr., Sect. E: Cryst. Struct. Rep. Online*, 2007, **63**, i167.
25 B. A. Demko, K. Eichele and R. E. Wasylishen, *J. Phys. Chem. A*, 2006, **110**, 13537.
26 A. Müller, B. Krebs and H. Beyer, *Z. Naturforsch., B*, 1968, **23**, 1537.
27 S. Schramm and E. Oldfield, *J. Am. Chem. Soc.*, 1984, **106**, 2502.
28 J. Skibsted, N. C. Nielsen, H. Bildsøe and H. J. Jakobsen, *Chem. Phys. Lett.*, 1992, **188**, 405.

